Effect of Tb substitution on the magnetic properties of exchange-biased $Nd_2Fe_{14}B/Fe_3B$

S. Manjura Hoque · M. A. Hakim · F. A. Khan · N. H. Dan

Abstract Tb-substituted $(Nd,Tb)_2Fe_{14}B/Fe_3B$ nanocomposite ribbons have been synthesized by melt spinning of $Nd_3Tb_1Fe_{76}Cu_{0.5}Nb_1B_{18.5}$ alloys. Tb substitution has significantly enhanced the value of coercivity and Curie temperature. Highest value of coercivity has been obtained as 4.76 kOe for the sample annealed at 953 K for 10 min. Curie temperature of Tb substituted sample, $Nd_3Tb_1Fe_{76}Cu_{0.5}Nb_1B_{18.5}$ is 549 K while Curie temperature of the sample without Tb, $Nd_4Fe_{76}Cu_{0.5}Nb_1B_{18.5}$ is 535 K. Recoil hysteresis loops measured along the major demagnetization curve are steep having small recoil loop area. Temperature dependence of coercivity, remanent ratio and maximum energy product have been measured for the sample annealed at 893 K and 923 K for 10 min. At 5 K, coercivity and maximum energy product of the sample annealed at 893 K for 10 min are 5.2 kOe and 11.5 MGOe respectively and the sample annealed at 923 K for 10 min are 6 kOe and 13.1 MGOe respectively.

Introduction

Nd-deficient $Nd_2Fe_{14}B/Fe_3B$ based nanocomposite alloys are characterized by their exchange-spring behavior resulting in remanent ratio > 0.5, which is highly desirable for permanent magnet development. Magnetic properties of exchange spring magnets are governed by the soft and hard magnetic phases that develop under appropriate annealing condition. High reduced remanence characteristic to these materials arises from exchange coupling of magnetic moments across the interface between two phases. Besides high reduced remanence such systems possess high energy product $(BH)_{max}$ and a reversible demagnetization curve, which has been called as exchange-spring behavior. This causes the magnetic moments of both the phases to remain in the same direction. It has been demonstrated earlier by Kneller and Hawig [1] that the enhancement of remanence and coercivity by this mechanism is mainly governed by the crystallite sizes of both the phases in particular the soft phase, which can be controlled by dopants and/or additives and also by controlling heat treatment. Compared to single phase $Nd_2Fe_{14}B$, nanocomposite $Nd_2Fe_{14}B/Fe_3B$ based alloys are economic and corrosion resistant. Various dopants and substituents have been used to enhance the value of coercivity. A partial substitution of Nd by heavy rare earth elements like Tb increases the anisotropy field, H_A which enhances the coercive field, but decreases strongly the remanence due to its antiferromagnetic coupling between rare earth and the transition metal [2]. Tb addition has previously been used to increase the coercivity of $Pr_2Fe_{14}B$ due to higher anisotropy field of $Tb_2Fe_{14}B$ [3].

Studies [4–6] of macroscopic reversible and irreversible magnetic behavior in nano-crystalline exchange coupled two-phase permanent magnetic materials demonstrate relatively steep recoil curves, which possess recoil permeabilities five times greater than those in conventional sintered magnets [1]. By using the demagnetization remanence (DCD) technique it has been demonstrated that when a negative field (lower than the critical field for magnetization

S. M. Hoque (✉) · M. A. Hakim
Materials Science Division, Atomic Energy Center, Dhaka 1000, Bangladesh
e-mail: manjura_hoque@yahoo.com

F. A. Khan
Department of Physics, Bangladesh University of Engineering and Technology, Dhaka 1000, Bangladesh

N. H. Dan
Institute of Materials Science, Vietnamese Academy of Science and Technology, Hanoi, Vietnam

reversal of the hard phase) is applied on a previously saturated sample, a near reversible rotation of magnetization of the soft phase is obtained when the field is decreased back to zero giving rise to the high recoil permeability.

The aim of the present work is to obtain nanocomposite $(NdTb)_2Fe_{14}B/Fe_3B$ magnets with higher coercvity evolved from the composition of $Nd_3Tb_1Fe_{76}Cu_{0.5}Nb_1B_{18.5}$ with the variation of annealing temperature and time. In this composition, Cu and Nb controls microstructure. For the optimized annealed sample reversible and irreversible component of magnetization have been studied by recoil hysteresis and DCD technique. Temperature dependence of coercivity, remanent ratio and maximum energy product have been measured for the sample annealed at 893 K and 923 K for 10 min between 5 K and 380 K.

Experimentals

An ingot of composition $Nd_3Tb_1Fe_{76}Cu_{0.5}Nb_1B_{18.5}$ was prepared by arc melting the constituent elements in an argon atmosphere. The purity and origin of the materials were Fe (99.98%), Cu (99+%), Nb (99.8%), B (99.5%), Si (99.9%), Nd (99.9%), Tb (99.9%) from Johnson Matthey (Alfa Aesar). Amorphous ribbons were prepared from the ingot using a melt spin machine with a wheel speed of 25 m/s in an Ar atmosphere. The resulting ribbons were heat treated in an evacuated quartz tube of 10^{-5} mbar pressure at different temperatures and holding time to observe the effect of annealing condition on the magnetic properties. Differential Scanning Calorimetry was used to determine the crystallization temperature and x-ray diffraction (CuK_α) was used to identify the phases present in the samples at different stages of the crystallization process. Magnetization measurements were performed by Quantum Design MPMSXL5 Superconducting Quantum Interference Device (SQUID) magnetometer.

Results and discussion

Crystallization temperature of $Nd_3Tb_1Fe_{76}Cu_{0.5}Nb_1B_{18.5}$ was identified by differential thermal analysis (DTA). The DTA trace shown in Fig. 1 has been measured on a sample in the as-cast condition by carrying out measurement in nitrogen atmosphere with a continuous heating rate of 20 K/min. The curve shows exothermic peaks which represents the formation of both soft and hard phases. Onset of crystallization of the first exothermic peak is at 843 K while peak temperature is at 860 K. For the second exothermic peak, the peak temperature is at 887 K. In order to determine crystallization products at different stages of crystallization x-ray diffraction studies have been performed.
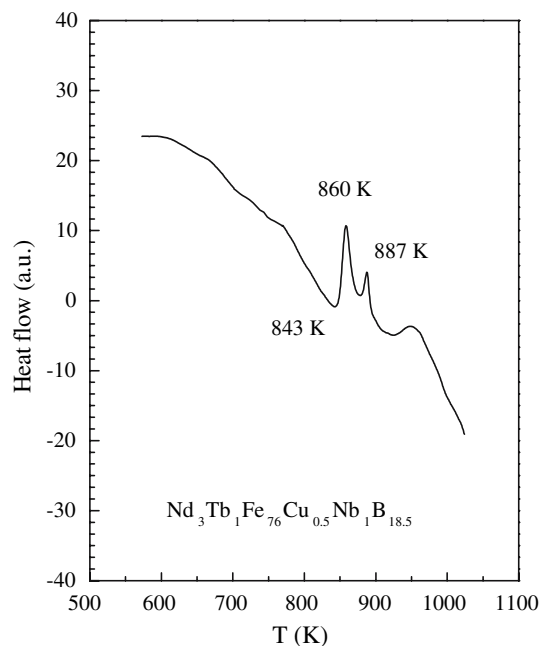

Fig. 1 DTA trace of $Nd_{3.5}Tb_1Fe_{76}Cu_{0.5}Nb_{1.2}B_{18.5}$ in the as-cast condition with a heating rate of 20 K/min

X-ray diffraction patterns of the samples annealed at 853 K, 873 K, 893 K, and 923 K for 10 min are shown in Fig. 2. For the annealing temperature of 853 K, soft phase Fe_3B has formed. For the higher annealing temperature of
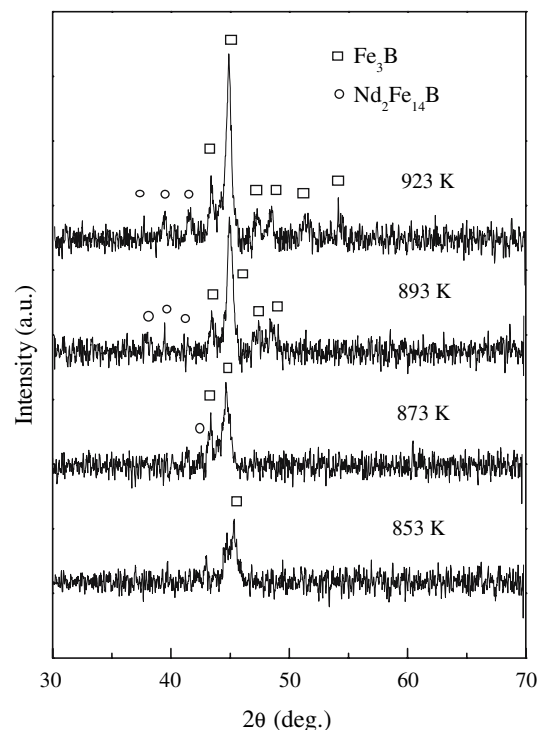

Fig. 2 X-ray diffraction pattern of $Nd_3Tb_1Fe_{76}Cu_{0.5}Nb_1B_{18.5}$ samples in the annealed condition

Table 1 Hysteresis loop parameters for $Nd_3Tb_1Fe_{76}Cu_{0.5}Nb_1B_{18.5}$

Annealing temperature, K	Annealing time, min	M_m emu/g	H_c kOe	M_r/M_s	$(BH)_{max}$ MGOe	g.s. nm
853	10	147	–	–	–	10
873	10	146	2.68	0.719	6.11	14
893	10	142	4.10	0.697	7.85	14
913	10	147	4.00	0.665	7.26	13
923	10	147	4.40	0.683	9.43	14
953	10	147	4.76	0.674	8.67	15

873 K, hard magnetic phase $Nd_2Fe_{14}B$ has formed in a small amount in association with the soft phase Fe_3B. At higher annealing temperature of 893 K and 923 K characteristic patterns of the mixture of soft and hard phases (Fe_3B and $Nd_2Fe_{14}B$) are observed. With the increase of annealing temperature grain size does not change significantly and remains on the average of 14 nm as determined from FWHM of highest intensity peak and presented in Table 1. But the relative amount of soft and hard phases change with the increase of annealing temperature as can be observed from the relative intensity of soft and hard phases.

Hysteresis loops obtained at different annealing temperatures have been presented in Fig. 3. In Fig. 3, y-axis values have been normalized by the maximum value of saturation magnetization. It may be noticed that saturation magnetization has not been achieved even after applying a maximum field of 3 T. This is due to the high magneto-crystalline anisotropy which is common for $R_2Fe_{14}B$.

Values of maximum magnetization, coercivity, remanent ratio, and maximum energy product derived from the hysteresis loops have been presented in Table 1. While varying annealing temperature, coercivity generally increases with the increase of annealing temperature while remanent ratio decreases. Highest value of energy product about 9.43 MGOe has been obtained for the sample annealed at 923 K for 10 min. In Fig. 3, there is no change in the shape of the hysteresis loops, which are convex like single phase permanent magnet up to the annealing temperature of 953 K. This indicates that the material is exchange-coupled up to the annealing temperature adopted in this experiment.

In Fig. 4, hysteresis loops of samples of compositions $Nd_3Tb_1Fe_{76}Cu_{0.5}Nb_1B_{18.5}$ and $Nd_4Fe_{76}Cu_{0.5}Nb_1B_{18.5}$ have been presented. It is seen from Table 1 that the highest value of $(BH)_{max}$ of $Nd_3Tb_1Fe_{76}Cu_{0.5}Nb_1B_{18.5}$ has been obtained for the sample annealed at 923 K for 10 min. In Fig. 4, the sample of composition $Nd_4Fe_{76}Cu_{0.5}Nb_1B_{18.5}$ annealed at the same temperature i.e. 923 K for 10 min have been presented for comparison. Coercivity, remanent ratio and maximum energy product of $Nd_4Fe_{76}Cu_{0.5}Nb_1B_{18.5}$ are 3.18 kOe, 0.753 and 9.21 MGOe respectively. While the Coercivity, remanent ratio and maximum energy product of $Nd_3Tb_1Fe_{76}Cu_{0.5}Nb_1B_{18.5}$ are 4.40 kOe, 0.683 and 9.43 MGOe. Though an enhancement of coercivity takes place due to the higher anisotropy field when Nd is partially substituted by Tb, remanent ratio is decreased due to antiferromagnetic coupling between rare earth and transition metal [2]. The magnetization of light rare earth (LRE) sublattice couples ferromagnetically to the
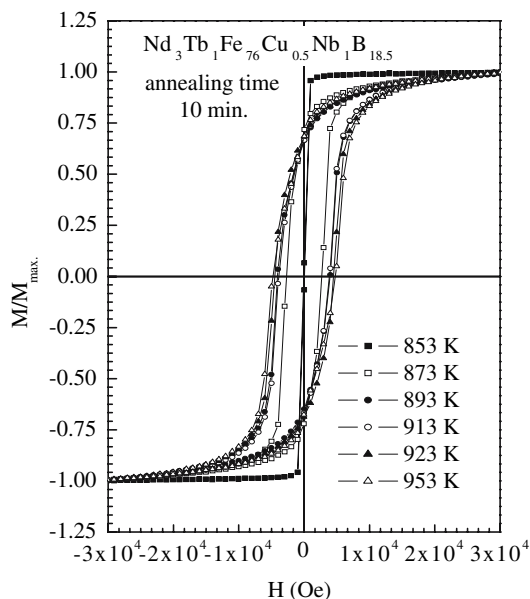
Fig. 3 Hysteresis loops of $Nd_3Tb_1Fe_{76}Cu_{0.5}Nb_1B_{18.5}$ samples in the annealed condition at different temperatures
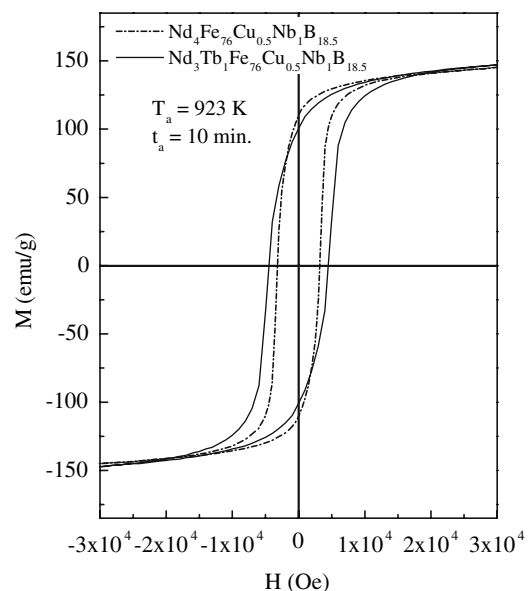
Fig. 4 Hysteresis loops of samples of compositions $Nd_3Tb_1Fe_{76}Cu_{0.5}Nb_1B_{18.5}$ and $Nd_4Fe_{76}Cu_{0.5}Nb_1B_{18.5}$
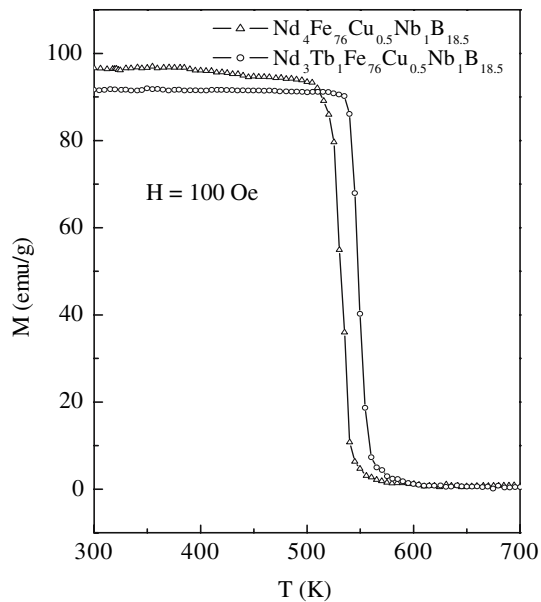
Fig. 5 Temperature dependence of magnetization of $Nd_3Tb_1Fe_{76}Cu_{0.5}Nb_1B_{18.5}$ and $Nd_4Fe_{76}Cu_{0.5}Nb_1B_{18.5}$ with an applied field of 100 Oe and heating rate of 20 K/min

Fig. 6 Recoil hysteresis loops for $Nd_3Tb_1Fe_{76}Cu_{0.5}Nb_1B_{18.5}$ sample annealed at 923 K for 10 min

magnetization of the transition metal sublattice. The opposite is true for the heavy rare earth (HRE) elements rendering these latter materials ferrimagnetic. It may be pointed out here that the anisotropy field of $Nd_2Fe_{14}B$ is 12 MA/m and $Tb_2Fe_{14}B$ is 28 MA/m [2]. Combined effect of antiferromagnetic coupling between Fe and Tb and higher anisotropy field of $Tb_2Fe_{14}B$ led to the enhancement of coercivity and reduction of remanent ratio, which in turn has resulted in lower value of energy product.

In Fig. 5, temperature dependence of magnetization has been presented with an applied field of 100 Oe and at a heating rate of 20 K/min for $Nd_3Tb_1Fe_{76}Cu_{0.5}Nb_1B_{18.5}$ and $Nd_4Fe_{76}Cu_{0.5}Nb_1B_{18.5}$. The characteristic feature of the curves is magnetization remains almost constant up to certain temperature followed by an abrupt decrease in its value passing though ferro-paramagnetic transition at the Curie temperature. The Curie temperature has been estimated from the rate of change of magnetization and found as 549 K for $Nd_3Tb_1Fe_{76}Cu_{0.5}Nb_1B_{18.5}$ and 535 K for $Nd_4Fe_{76}Cu_{0.5}Nb_1B_{18.5}$. Exchange in interaction between R and Fe moments enhances the Curie temperature [2].

Figure 6 shows room temperature (300 K) hysteresis loop and some minor recoil loops along the demagnetization branch for the sample annealed at 923 K for 10 min. In Fig. 7, the area of the recoil loops normalized to the area of half of the major hysteresis loop are plotted as a function of the reverse field H. The areas have been extracted by numerical integration of the recoil curves of Fig. 6. The development of the loop area is due to the decoupling of the magnetic moment between hard and soft phase. In
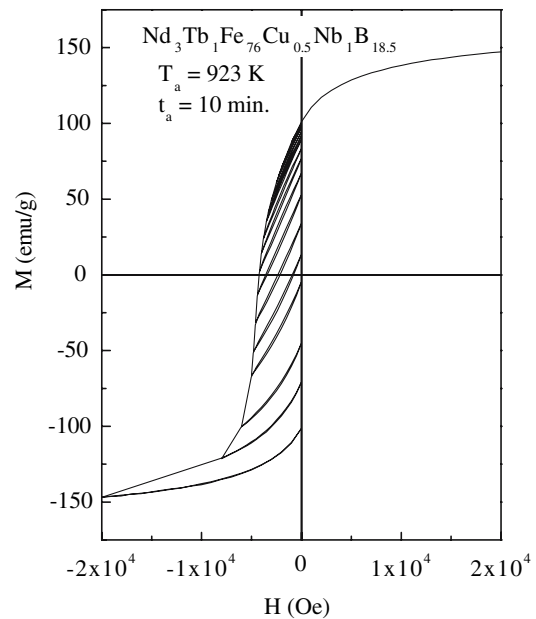
Fig. 7, the recoil area shows a pronounced maximum at the field where the largest number of hard phase grains switch magnetization direction. This field amounts to 4,600 Oe for the sample annealed at 923 K for 10 min. As pointed out by Kang et al. [5], the peak in the recoil area is coincident with the coercivity of the hard component while the departure from zero recoil area at low reverse field corresponds to the inter-phase exchange field, H_{ex}.
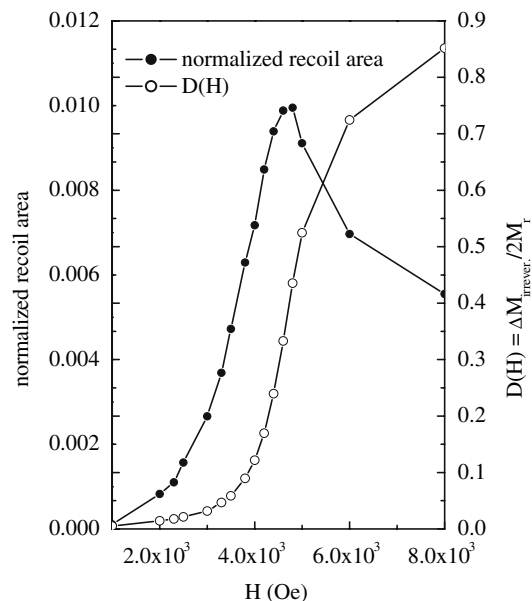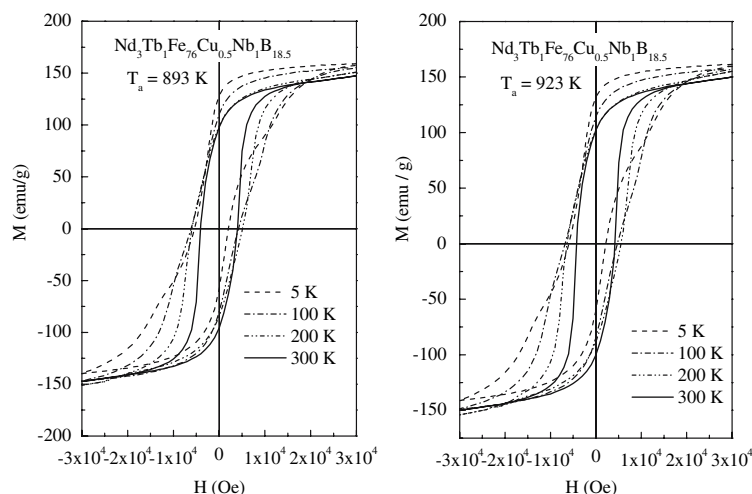

Fig. 7 Variation of irreversible component of magnetization $D(H)$ and normalized recoil area with reverse field

Fig. 8 Temperature dependence of hysteresis loops for samples annealed at 893 K and 923 K

In Fig. 7, the reduced quantity $D(H) = [M_r - M_d(H)]/2M_r = -\Delta M_{irrev}(H)/2M_r$ is plotted vs. reverse field H, where $M_d(H)$ is the dc field demagnetization remanence i.e. the remanence acquired after saturation in one direction and subsequent application of a dc field H in the opposite direction and M_r is the saturation remanence. The curves of Fig. 7 provide information about the stability of the reversible state and about the critical field of irreversible changes of the magnetization. For the sample annealed at 923 K, the $D(H)$ vs. H curve is characterized by relatively sharp change of $D(H)$ at the critical field where irreversible change in the hard phase is relatively large, which has been obtained from the derivative of the $D(H)$ vs. H curve and found as 4,000 Oe.

Temperature dependence of the hysteresis loop has been measured in the temperature range of 5 K to 380 K for the sample annealed at 893 K and 923 K. Some representative hysteresis loops are shown in Fig. 8 and derived hysteresis loop parameters for all measured temperatures are plotted in Fig. 9. The shape of the hysteresis loop changes below 150 K, which is related to a spin re-orientation in the hard phase that occurs at low temperatures. From studies of powdered and single crystalline $Nd_2Fe_{14}B$, Givord et al. [7, 8] found that at temperatures below 135 K there is an angle θ between the easy magnetization direction and the c-axis that progressively increases and amounts to about 30° at low temperatures. Hadjipanayis et al. [9] observed that the hysteresis loop for $Nd_2Fe_{14}B/\alpha$-Fe becomes constricted below the spin reorientation temperature, i.e. with the decrease of temperature the magnetization curve becomes discontinuous at low field. The curves presented in Fig. 8 shows a change in the shape of the hysteresis loop below 150 K, which agree with the previous measurements [7–9].

In Fig. 9, temperature dependence of the coercivity, H_c, remanent ratio, M_r/M_s and maximum energy product, $(BH)_{max}$ are plotted. Curves for both the samples show
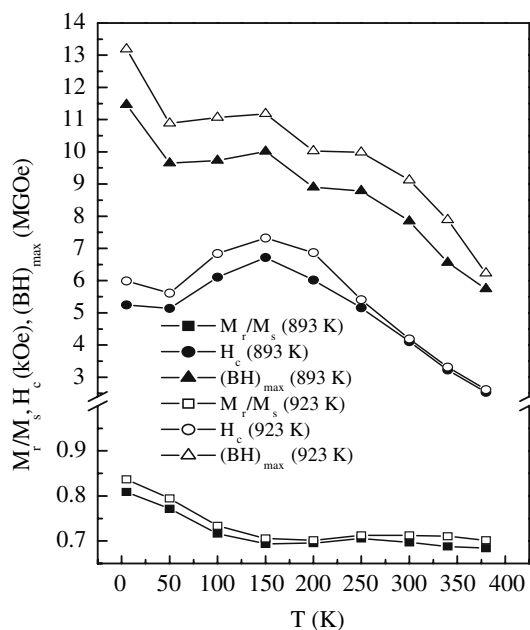

Fig. 9 Temperature dependence of hysteresis loop parameters for samples annealed at 893 K and 923 K for 10 min

similar behavior. Coercivity increases with the decrease of temperature up to about 150 K. Below 150 K there is a change of the slope of $H_c(T)$. Change of slope of $H_c(T)$ at low temperatures is related to the spin reorientation in the hard phase. This behavior of $H_c(T)$ may be compared with that reported in Ref. [10] in which a stronger decay of the coercivity at low temperatures is observed. The temperature dependence of remanent ratio, M_r/M is also governed by the temperature dependence of anisotropy field. The value of M_r/M_s decreases with the increase of temperature because of easier domain wall motion due to the reduction of the anisotropy field at higher temperature. Temperature dependence of maximum energy product, $(BH)_{max}$ also

decreases with the increase of temperature due to the reduction of anisotropy field for both samples.

Conclusions

A partial substitution of Nd by Tb led to the enhancement of coercive field up to a value of 4.76 kOe for the sample annealed at 953 K for 10 min. Recoil hysteresis loops are characterized by high recoil permeabilities and small recoil loop area, which indicates that the samples are exchange coupled. At low temperature, hysteresis loops are governed by the spin-reorientation of the easy axis of $Nd_2Fe_{14}B$. Below 200 K, field dependence of magnetization is discontinuous at low field leading to constricted hysteresis loop.

References

1. Kneller EF, Hawig R (1991) IEEE Trans Magn 27:3588
2. Sagawa M, Fujimura S, Yamamoto H, Matsuura Y (1984) IEEE Trans Magn Mag-20:1584
3. Jin ZQ, Okumura H, Hadjipanayis GC (2001) IEEE Trans Magn 37:2564
4. Harland CL, Lewis L-H, Chen Z, Ma B-M (2004) J Magn Mag Mater 271:53
5. Kang K, Lewis LH, Jiang JS, Bader SD (2005) J Appl Phys 98:113906
6. Withanawasam L, Hadjipanayis GC, Krause RF (1994) J Appl Phys 75:6646
7. Givord D, Tenaud P, Viadieu T (1986) J Appl Phys 60:3263
8. Givord D, Li HS, Perrier R (1984) Solid State Commun 51:857
9. Hadjipanayis GC, Hall C, Kim A (1987) IEEE Trans Magn 23:2533
10. Hadjipanayis GC, Withanawasam L, Krause RF (1995) IEEE Trans Magn 31:3596